

Effect of the Hydrophobicity to Net Positive Charge Ratio on Antibacterial and Anti-Endotoxin Activities of Structurally Similar Antimicrobial Peptides[†]

Yosef Rosenfeld, Naama Lev, and Yechiel Shai*

Department of Biological Chemistry, The Weizmann Institute of Science, Rehovot 76100, Israel

Received April 27, 2009; Revised Manuscript Received January 8, 2010

ABSTRACT: The interaction between host-defense antimicrobial peptides (AMPs) and the bacterial lipopolysaccharide (LPS) governs both the susceptibility of the bacteria to the peptide and the ability of the peptide to inhibit LPS activation of immune cells. Both functions depend on the biophysical properties of the peptides. However, the sequence and structural diversity of AMPs makes it difficult to determine common denominators required for antimicrobial and LPS neutralizing activities. Toward this end, we synthesized and investigated a series of nine 12-amino acid peptides and their fatty acid-conjugated analogues composed of both D- and L-isomers of Leu and Lys at various ratios. The positions of the D-amino acids were preserved. These peptides differ in their net positive charge and hydrophobicity. However, their overall structure in the membrane is similar, as determined by Fourier transform infrared spectroscopy. The peptides and their analogues were functionally tested for their antibacterial and hemolytic activity, their ability to permeate LPS vesicles, their ability to neutralize LPS activation of macrophages, and their effect on LPS morphology, determined by negative staining electron microscopy. The data revealed that increasing the ratio between hydrophobicity and the net positive charge increases both antimicrobial and LPS neutralization activities, but with different modes of contributions. Whereas antimicrobial activity increases linearly with the increase in the peptides' hydrophobicity, peptides with different hydrophobicities are endowed with similar LPS neutralizing activities. Besides adding important information regarding AMP parameters involved in antimicrobial and anti-LPS activities, this study suggests the use of such diastereomers as potential templates for the development of simple molecules that conduct both types of functions.

Antimicrobial peptides (AMPs) are evolutionarily ancient natural antibiotics, produced by all forms of life (1–3). Despite a vast diversity in their sequences, all of them show a specific or broad range of antimicrobial activities against bacteria, yeast, fungi, and viruses (3–5) (online sequences of all reported molecules can be found at <http://www.bbcm.univ.trieste.it/~tossi/antimic.html>). Accumulating data show that in addition to their direct antimicrobial activity, some linear AMPs have immunostimulatory, immunomodulatory, and anti-inflammatory activities (5–9). Others are capable of blocking the activation of immune cells induced by bacterial cell wall components such as lipopolysaccharide (LPS) in Gram-negative bacteria and lipoteichoic acid (LTA) in Gram-positive bacteria (10–15). The immune system has evolved to recognize LPS and LTA as pathogen-associated molecular patterns (PAMPs), which are released from bacteria after treatment with conventional antibiotics. Upon their recognition, LPS and LTA stimulate the innate immune cells, inducing the secretion of pro-inflammatory cytokines (e.g., TNF- α , IL1, and IL6), mainly by mononuclear cells and macrophages (16, 17). These cytokines can rapidly lead to the development of septic shock, which in extreme cases can cause death (18, 19). LPS can stimulate immune cells much better

than LTA, and therefore, it is an excellent target for in-depth studies for its interaction with LPS-neutralizing AMPs (20). However, the exact underlying mechanism and whether similar parameters are required for both antimicrobial and anti-LPS neutralizing activities are not yet well understood (21–25).

In limited cases, mostly studies with the cathelicidin family, it was reported that the peptides bind directly to the proteins of the LPS recognition signaling complex (6, 9, 11, 12, 26). Nevertheless, direct binding of the peptides to LPS or LTA is thought to be the main mechanism that prevents them from binding to the signaling complex (23, 27, 28).

The electrostatic interaction between cationic AMPs and the negatively charged LPS is the initial and rate-limiting step that governs both their antimicrobial and LPS neutralizing activities. For some AMPs, the LPS layer is a physical barrier that prevents them from reaching and permeating the inner membrane (27, 29–32), whereas others can overcome this barrier and traverse the inner membrane (33–36). Although the ability of the peptides to traverse the outer membrane is the main and initial step governing their antibacterial activity, most studies focused mainly on the interactions between the peptides and the model membranes that mimic the cytoplasmic membrane of the bacteria (37, 38). Limited studies on LPS–AMP interactions were investigated in the context of the ability of AMPs to neutralize the LPS endotoxic effect (23, 28, 39, 40). However, because of the diversity in the sequences and the structures of these peptides, it is difficult to extract specific criteria regarding the important parameters that govern the interaction between AMPs and LPS, which leads to LPS neutralization.

[†]This study was supported in part by the Jeanne and Joseph Nissim Foundation for Life Sciences Research. Y.S. is the incumbent of the Harold S. and Harriet B. Brady Professorial Chair in Cancer Research.

*To whom correspondence should be addressed: Department of Biological Chemistry, The Weizmann Institute of Science, Rehovot 76100, Israel. Telephone: 972-8-9342711. Fax: 972-8-9344112. E-mail: Yechiel.Shai@weizmann.ac.il.

Table 1: Designations, Sequences, and Relative Hydrophobicities of Peptides

| designation | sequence ^a | net charge | retention time ^b (min) | relative hydrophobicity ^c (% acetonitrile) |
|----------------------------------|--|------------|-----------------------------------|---|
| K ₅ L ₇ | <u>KKLLKLLKLLK</u> -NH ₂ | +6 | 27.5 | 38.75 |
| C6-K ₅ L ₇ | CH ₃ (CH ₂) ₄ CO-K <u>KKLLKLLKLLK</u> -NH ₂ | +5 | 32.6 | 46.4 |
| C8-K ₅ L ₇ | CH ₃ (CH ₂) ₆ CO-K <u>KKLLKLLKLLK</u> -NH ₂ | +5 | 34.7 | 49.5 |
| K ₇ L ₅ | <u>KKLLKLLKLLK</u> -NH ₂ | +8 | 22.1 | 30.65 |
| C6-K ₇ L ₅ | CH ₃ (CH ₂) ₄ CO-K <u>KKLLKLLKLLK</u> -NH ₂ | +7 | 26 | 36.5 |
| C8-K ₇ L ₅ | CH ₃ (CH ₂) ₆ CO-K <u>KKLLKLLKLLK</u> -NH ₂ | +7 | 28 | 39.5 |
| K ₉ L ₃ | <u>KKLLKLLKLLK</u> -NH ₂ | +10 | 16.5 | 22.25 |
| C6-K ₉ L ₃ | CH ₃ (CH ₂) ₄ CO-K <u>KKLLKLLKLLK</u> -NH ₂ | +9 | 19.8 | 27.2 |
| C8-K ₉ L ₃ | CH ₃ (CH ₂) ₆ CO-K <u>KKLLKLLKLLK</u> -NH ₂ | +9 | 22.1 | 30.65 |

^aAll peptides are amidated at their C-termini. Fatty acids are attached to the N-termini of the peptides. Underlined and bold letters represent D-amino acids. ^bRP-HPLC retention time in the C18 column by using a gradient of 5 to 65% acetonitrile in water for 40 min. ^cRelative hydrophobicity is reflected by the percent of acetonitrile at the retention time.

Here we investigated the contribution of the net positive charge and hydrophobicity to LPS neutralizing and antimicrobial activities of a group of structurally similar AMPs. This group includes a new series of 12-mer peptides composed of D,L-amino acids and their fatty acid conjugates. The peptides were investigated functionally for their antimicrobial, hemolytic, and LPS neutralizing activities. Their mode of interaction with LPS was determined by using various biophysical methods, including fluorescence, Fourier transform infrared (FTIR), and negative staining electron microscopy. The results are discussed in connection with the contribution of the net positive charge and the hydrophobicity of the peptides in bestowing them with the two activities: bactericidal and LPS neutralizing.

MATERIALS AND METHODS

Materials. Rink amide MBHA resin, 4-methylbenzhydrylamine resin (BHA), and 9-fluorenylmethoxycarbonyl (Fmoc) amino acids were obtained from Calbiochem-Novabiochem AG. Hexanoic acid and caprylic (octanoic acid) were purchased from Sigma Chemical Co. Other reagents used for peptide synthesis included trifluoroacetic acid (TFA) (Sigma), piperidine (Merck), *N,N*-diisopropylethylamine (DIEA) (Sigma), *N*-methylmorpholine (NMM) (Fluka), *N*-hydroxybenzotriazole hydrate (HOBT) (Aldrich), 2-(1*H*-benzotriazol-1-yl)-1,1,3,3-tetramethyluronium hexafluorophosphate (HBTU), and dimethylformamide (DMF, peptide synthesis grade) (Biolab). Lipopolysaccharide from *Escherichia coli* O111:B4 (LPS) was purchased from Sigma. Potential sensitive dye diS-C₃-5 was purchased from Molecular Probes (Eugene, OR). Tissue culture medium, serum, antibiotics, and supplements were purchased from Biological Industries (Beit Haemek, Israel).

Peptide Synthesis, Acylation, and Purification. Peptides were synthesized by a 9-fluorenylmethoxycarbonyl (Fmoc) solid-phase method on Rink amide MBHA resin, by using an ABI 433A automatic peptide synthesizer (for the list of the peptides, see Table 1). The lipophilic acid was attached to the N-terminus of a resin-bound peptide by standard Fmoc chemistry. Briefly, after removal of the Fmoc from the N-terminus of the peptide with a solution of 20% piperidine in DMF, the fatty acid (7 equiv, 1 M in DMF) was coupled to the resin under similar conditions used for the coupling of an amino acid. The peptides were cleaved from the resin with 95% TFA and were purified by reverse-phase high-performance liquid chromatography (RP-HPLC) on a C18 Bio-Rad semipreparative column (250 mm × 10 mm, 300 Å pore size, 5 μm particle size). The purified peptides were found to be homogeneous (>98%) by analytical RP-HPLC. Electrospray

mass spectroscopy was used to confirm their molecular weight, and amino acid analysis was used to confirm the composition of the peptidic moiety.

Antimicrobial Activity. The antibacterial activity of the peptides was examined in sterile 96-well plates (Nunc F96 microtiter plates) in a final volume of 100 μL as follows. Aliquots (50 μL) of a suspension containing bacteria (midlog phase) at a concentration of 10⁶ colony-forming units/mL in culture medium (LB medium) were added to 50 μL of doubly distilled water (DDW) containing the peptide in serial 2-fold dilutions in DDW. After incubation for 18–20 h at 37 °C, inhibition of growth was assessed by measuring the absorbance at 600 nm with a Microplate autoreader EL309 (Biotek Instruments). The antibacterial activities were expressed as the minimal inhibitory concentration (MIC), the concentration at which 100% inhibition of growth was observed after incubation for 18–20 h. The bacteria used were *E. coli* D21, *E. coli* O111:B4, *E. coli* O26:B6, *Acinetobacter baumannii* ATCC 19606, *Pseudomonas aeruginosa* ATCC 27853, and *Staphylococcus aureus* ATCC 6538P.

Hemolytic Activity. Fresh hRBCs were rinsed three times with PBS [35 mM phosphate buffer and 0.15 M NaCl (pH 7.3)] by centrifugation for 10 min at 800g and resuspended in PBS. The peptides dissolved in PBS were then added to 50 μL of the stock hRBC solution in PBS to create a final volume of 100 μL [final erythrocyte concentration of 4% (v/v)]. The resulting suspension was incubated with agitation for 60 min at 37 °C. The samples were then centrifuged at 800g for 10 min. By measuring the absorbance of the supernatant at 540 nm, we monitored the release of hemoglobin. Controls for zero hemolysis (blank) and 100% hemolysis consisted of hRBCs suspended in PBS and 1% Triton X-100, respectively.

Evaluation of Secretion of TNF-α from RAW264.7 Macrophages. RAW264.7 macrophages were cultured overnight in 96-well plates (2 × 10⁵ cells/well). The medium was then removed, followed by the addition of fresh medium to each well. The cells were stimulated with LPS (10 ng/mL) in the absence or presence of the different peptides (K₅L₇, K₇L₅, or K₉L₃) at 0.5, 1, or 5 μM and their lipopeptide derivatives. Untreated cells served as controls. The cells were incubated for 6 h at 37 °C; thereafter, samples of the medium from each treatment were collected. The TNF-α concentrations in the samples were evaluated using the mouse TNF-α enzyme-linked immunosorbent assay (ELISA) kit according to the manufacturer's protocol (BIOSOURCE, USA). All experiments were conducted in duplicate.

LPS Destabilization Induced by the Peptides. Membrane destabilization, which results in the collapse of the diffusion

potential, was detected fluorimetrically as described previously (31). Briefly, a LPS large unilamellar vesicle (LUV) suspension (10 mg/mL in 200 μ L) prepared in K^+ buffer [50 mM K_2SO_4 and 25 mM HEPES-sulfate (pH 6.8)] was added to an isotonic K^+ -free buffer [50 mM Na_2SO_4 and 25 mM HEPES-sulfate (pH 6.8)] to a final concentration of 50 μ g/mL LPS in 10 mL, and then the dye 3,3'-dipropylthiadicarbocyanine iodide (di-S-C3-5) was added. The subsequent addition of valinomycin (0.1 μ M) created a negative diffusion potential inside the vesicles by the selective efflux of K^+ ions, which resulted in quenching of the dye fluorescence ($\Delta\psi = -142$ mV). The LPS solution was added to serial dilutions of each of the peptides in K^+ -free buffer. Peptide-induced membrane permeation for all of the ions in the solution caused the diffusion potential to dissipate, manifested by an increase in fluorescence. The fluorescence was monitored using excitation and emission wavelengths of 620 and 670 nm, respectively.

FTIR Analysis of the Structures of the Peptides. To determine the influence of LPS on the secondary structure of the peptides, we used attenuated total reflectance Fourier transform infrared (ATR-FTIR) spectroscopy. Spectra were recorded with a Bruker equinox 55 FTIR spectrometer equipped with a deuterated triglyceride sulfate detector coupled to an ATR device as previously described (23, 41). Briefly, prior to sample preparations, the TFA counterions, which associate with the peptides, were replaced with chloride ions through several lyophilizations of the peptides in 0.1 M HCl to eliminate an absorption band near 1673 cm^{-1} . After the ion exchange, the peptides (final concentration of 100 μ g/mL) were dissolved in 400 μ L of LPS solution in DDW (250 μ g/mL), deposited on a ZnSe horizontal ATR prism, and dried under vacuum at 37 $^{\circ}C$. Spectra were recorded, and the respective pure LPS spectra were subtracted to yield the difference in the spectra. The background for each spectrum was a clean ZnSe prism. Hydration of the sample was achieved via introduction of excess deuterium oxide (2H_2O) into a chamber placed on top of the ZnSe prism in the ATR casting, and incubation for 15 min before the spectra were recorded. The H–D exchange was considered complete after a total shift of the amide II band. Any contribution of atmospheric vapor and the LPS to the absorbance spectra near the amide I peak region of the peptides was eliminated via subtraction of the spectra of pure LPS equilibrated under the same conditions as the sample in LPS.

ATR-FTIR Data Analysis. Prior to curve fitting, a straight baseline passing through the ordinates at 1700 and 1600 cm^{-1} was subtracted. To resolve overlapping bands, we processed the spectra using PEAKFIT (Jandel Scientific, San Rafael, CA). Second-derivative spectra were calculated to identify the positions of the component bands in the spectra. These wavenumbers were used as initial parameters for curve fitting with Gaussian component peaks. Positions, band widths, and amplitudes of the peaks were varied until (i) the resulting bands shifted by no more than 2 cm^{-1} from the initial parameters, (ii) all the peaks had reasonable half-widths (< 20 – 25 cm^{-1}), and (iii) there was good agreement between the calculated sum of all the components and the experimental spectra ($r^2 > 0.99$). We estimated the relative contents of the different secondary structure elements by dividing the areas of individual peaks, assigned to a specific secondary structure, by the whole area of the resulting amide I band. The results of two independent experiments were averaged.

Electron Microscopy (EM). Samples containing *E. coli* O111:B4 (1×10^6 CFU/mL) in PBS were incubated with peptides (100 μ M) for 60 min. A drop containing the bacteria was deposited onto a carbon-coated grid and negatively stained with 2%

phosphotungstic acid (PTA) (pH 6.8). In another experiment, LPS suspended in PBS (1 mg/mL) was incubated for 1 h with each of the peptides at 100 μ M. The LPS suspension that was not incubated with the peptides served as a control. A drop from each treatment was deposited onto a carbon-coated grid and negatively stained with uranyl acetate (1%). Finally, a drop of solution from each of the peptides in PBS (100 μ M) was deposited onto a carbon-coated grid and negatively stained with 2% PTA (pH 6.8). The grids were examined on a JEOL JEM 100B electron microscope (Japan Electron Optics Laboratory Co., Tokyo, Japan).

RESULTS

Antibacterial and Hemolytic Activity of the Peptides and Lipopeptides. The antibacterial activities of the peptides and their fatty acid-conjugated derivatives were tested against five Gram-negative bacterial strains and one representative Gram-positive strain, and the results are summarized in Table 2. The data reveal two groups. The first group includes the barely active K_7L_5 , K_9L_3 , and the two fatty acid derivatives ($C_6-K_9L_3$ and $C_8-K_9L_3$), and the second group includes the active K_5L_7 , $C_6-K_5L_7$, $C_8-K_5L_7$, $C_6-K_7L_5$, and $C_8-K_7L_5$. The general trend is that increasing the hydrophobicity of the peptide either by substituting lysines for leucines (K_5L_7 vs K_7L_5) or by coupling a short fatty acid strongly improves the antibacterial activity. The peptides were also tested for their hemolytic activity against hRBCs. The data revealed practically no hemolytic activity at elevated concentrations (100 μ M) for all peptides besides $C_8-K_5L_7$, which exhibited only 19% activity at high concentrations.

Effect of the Peptides on the Morphology of Bacteria As Visualized by Negative Staining Electron Microscopy. We added three representative peptides and lipopeptides, namely, K_5L_7 , $C_8-K_5L_7$, and $C_8-K_9L_3$, to *E. coli* O111:B4 cells and followed changes in the morphology of bacteria (Figure 1). In agreement with the antimicrobial assay results, $C_8-K_5L_7$ was the only highly active peptide. It caused complete disruption of the bacterial membrane followed by leakage of the cytoplasm content. Note that with $C_8-K_9L_3$, the bacteria are not damaged but are surrounded by a “cloudlike” material. As seen in Figure 6, this material most probably consists of micelles of $C_8-K_9L_3$. This suggests that the most active peptide, $C_8-K_5L_7$, has a detergent-like activity.

LPS Detoxification by the Peptides. The ability of the peptides to inhibit the LPS endotoxic effect was determined by following the TNF- α concentration secreted by LPS-stimulated macrophages that were incubated with the peptides at different concentrations (Figure 2). Similar to the results of the antibacterial assay, K_9L_3 and its two lipopeptidic derivatives could not neutralize LPS-stimulated activation of macrophages. In contrast, the other peptides and lipopeptides were active, although with various potencies. Compared with the unmodified peptides K_5L_7 and K_7L_5 , which had similar and low activity only at the highest concentration tested (5 μ M peptide), all of their fatty acid derivatives, namely, $C_6-K_5L_7$, $C_8-K_5L_7$, $C_6-K_7L_5$, and $C_8-K_7L_5$, were highly active.

LPS Permeation Induced by the Peptides. The peptides and lipopeptides were tested for their ability to dissipate the diffusion potential in LPS LUVs as a measure of their potential to permeate LPS. The data revealed that within each subgroup, the longer the fatty acid, the stronger the activity (Figure 3). The most active group includes $C_6-K_5L_7$ and $C_8-K_5L_7$; the second group with moderate activity includes K_5L_7 , $C_6-K_7L_5$, and $C_8-K_7L_5$, and the third group, which is inactive, includes unmodified K_7L_5 and K_9L_3 and its fatty acid derivatives.

Table 2: Antibacterial^a and Hemolytic Activities of the Peptides

| | <i>E. coli</i> O111:B4 | <i>E. coli</i> D21 | <i>E. coli</i> O26:B6 | <i>A. baumannii</i> ATCC 19606 | <i>P. aeruginosa</i> ATCC 27853 | <i>S. aureus</i> ATCC 6538P | % hemolysis (at 100 μ M) |
|----------------------------------|------------------------|--------------------|-----------------------|--------------------------------|---------------------------------|-----------------------------|------------------------------|
| K ₅ L ₇ | 25 | 33 | 25 | 50 | 37.5 | 37.5 | 0 |
| C6-K ₅ L ₇ | 12.5 | 6.25 | 12.5 | 10 | 10 | 6.25 | 0 |
| C8-K ₅ L ₇ | 6.25 | 4.5 | 6.25 | 4.5 | 3 | 3.12 | 19 |
| K ₇ L ₅ | 50 | 50 | 50 | > 100 | > 100 | > 100 | 0 |
| C6-K ₇ L ₅ | 25 | 25 | 12.5 | 37.5 | 37.5 | 50 | 0 |
| C8-K ₇ L ₅ | 12.5 | 10 | 6.25 | 19 | 15 | 20 | 0 |
| K ₉ L ₃ | 50 | 50 | 50 | > 100 | > 100 | > 100 | 0 |
| C6-K ₉ L ₃ | 50 | 50 | 50 | 100 | 100 | 100 | 0 |
| C8-K ₉ L ₃ | 50 | 50 | 50 | 50 | 50 | 100 | 0 |

^aThe antimicrobial activity is represented by the average minimal inhibitory concentration (MIC, in micromolar).

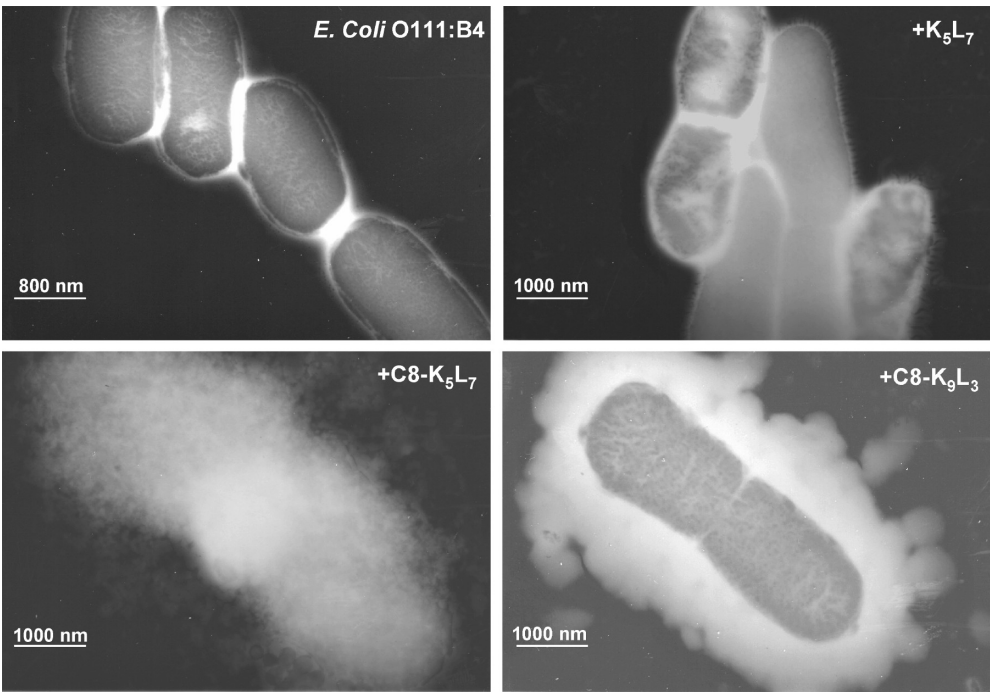


FIGURE 1: Visualizing the effect of the peptides on intact bacteria. Electron micrographs of negatively stained bacteria treated with different peptides. All samples were negatively stained with 2% phosphotungstic acid (pH 6.8).

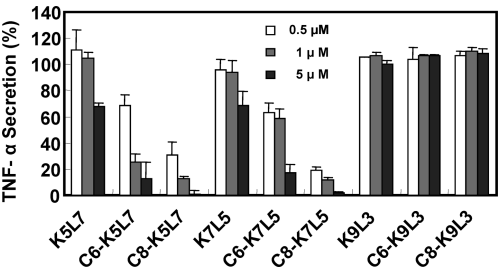


FIGURE 2: Effect of the peptides and lipopeptides on TNF- α secretion by macrophages stimulated with LPS. RAW264.7 macrophages were stimulated with LPS (10 ng/mL) in the absence or presence of each of the different peptides at 0.5, 1, or 5 μ M. After 6 h, medium samples were evaluated for their TNF- α concentrations with an ELISA. The results represent the percentage of TNF- α secretion normalized to cells that were stimulated with LPS only. Untreated cells served as controls. The results represent the average of three independent experiments, each performed in duplicate. Bars represent the standard deviation.

Correlation between Hydrophobicity and Functions. Figure 4 shows a correlation between the relative hydrophobicity

of the peptides (as reflected by the percentage of acetonitrile required to elute the peptide from the hydrophobic C18 column) and their three different functions: (i) their antibacterial activity, as reflected by the mean of their MICs against all Gram-negative bacteria strains that were tested (panel A); (ii) their ability to dissipate the LPS LUV diffusion potential (panel B); and (iii) their activity (at 5 μ M) in neutralizing endotoxin, as reflected by the percentage of inhibition of LPS-induced TNF- α secretion (panel C). The data revealed that although both antimicrobial and LPS neutralizing activities show a similar trend, meaning that higher activity correlates with higher hydrophobicity, the patterns of these correlations are different (Figure 4). There is a linear correlation between the increase in the relative hydrophobicity and improved antibacterial activity, which is reflected by lower MIC values (Figure 4A) ($R^2 = 0.87$). In comparison, the anti-endotoxic activity shows a weak trend with more scatter (Figure 4C). Peptides with similar hydrophobicities have significant differences in their LPS neutralizing activities (K₅L₇ and C8-K₇L₅), and peptides with the same activity have significant differences in their hydrophobicities (K₅L₇ and K₇L₅, C6-K₅L₇ and C6-K₇L₅, and C8-K₅L₇ and C8-K₇L₅).

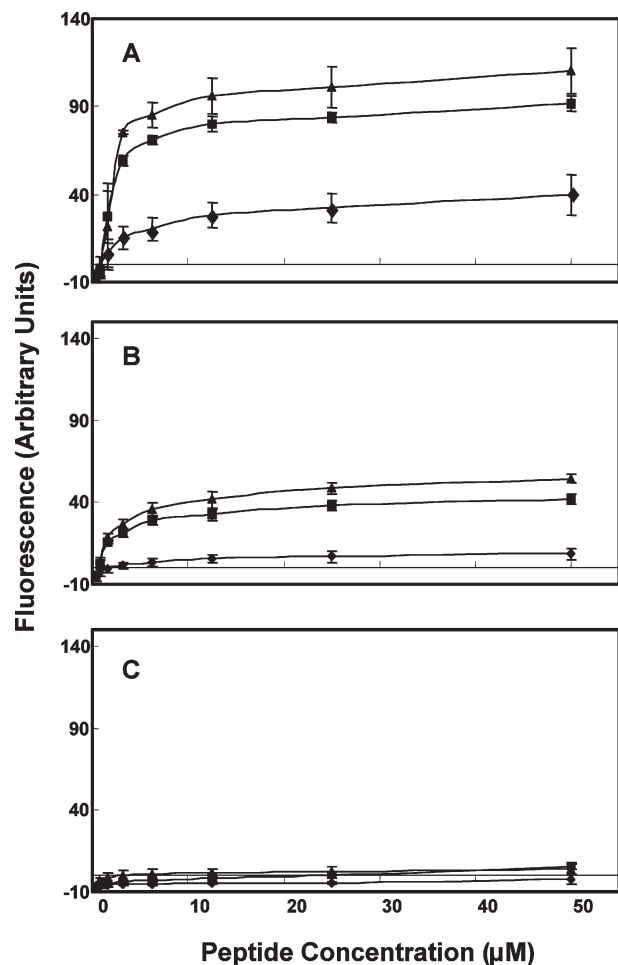


FIGURE 3: Effect of the concentrations of different peptides on the diffusion potential induced in LPS LUVs. The effect of the peptides on the diffusion potential was followed by monitoring the changes in the fluorescence of the potential sensitive dye diS-C₃-5. (A) K₅L₇ peptides, (B) K₇L₅ peptides, and (C) K₉L₃ peptides: (◆) nonconjugated peptides, (■) peptides conjugated to hexanoic acid, and (▲) peptides conjugated to octanoic acid. The results represent the average of two independent experiments each performed in duplicate. Bars represent the standard deviation.

Figure 4B shows a linear correlation ($R^2 = 0.92$) between the experimental hydrophobicity and the activity of the peptides in the dissipation of diffusion potential experiments. This curve is similar to that obtained for the MICs (Figure 4B). Note that the absolute values of the slopes of the curves are similar (0.30 and 0.26 for the antimicrobial and dissipation of diffusion potential, respectively). The slopes of the curves are inverted, since high antimicrobial activity is reflected by low MICs, whereas high LPS permeating activity is reflected by a high percentage of leakage.

Overall, the data indicate a direct relationship between the increase in antimicrobial activity and the ability of the peptides to traverse the LPS barrier, but not with LPS neutralizing activity, which seems to be dependent on a threshold of hydrophobicity. Once this hydrophobicity is reached, it is concomitant with potent, LPS neutralizing activity.

Structure of the Peptides Bound to LPS As Determined by FTIR Spectroscopy. We used FTIR spectroscopy to determine the secondary structure components of the peptides when they are bound to LPS. We have shown in previous studies that the assignment of structural components of D,L-amino acid peptides by using FTIR spectroscopy and the appropriate wavenumbers gives results that agree with NMR-derived

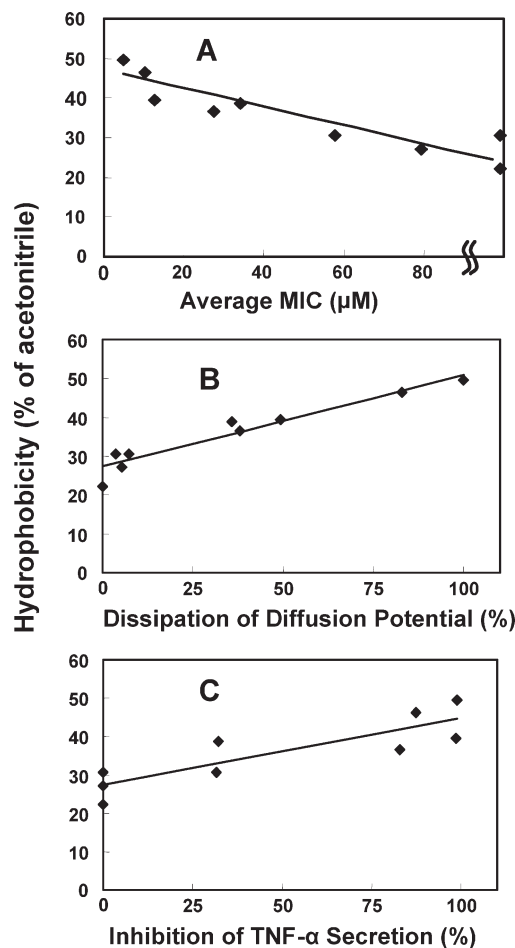


FIGURE 4: Effect of hydrophobicity of the peptides on their biological activities. The relative hydrophobicity of the peptides [as reflected by the percentage of acetonitrile required to elute the peptide from the hydrophobic C18 column (Table 1)] was extrapolated against (A) their antibacterial activity, as reflected by the mean of their MICs against all Gram-negative bacteria that were tested, (B) the ability of the peptides to dissipate LPS LUV diffusion potential, and (C) the activity of the peptides in neutralizing endotoxin as reflected by the percent inhibition of LPS-induced TNF- α secretion by the peptides.

structures (42, 43). In buffer, all the peptides and lipopeptides did not show significant signals that could be deconvoluted and therefore are not shown. Note that satisfactory signals can be obtained in solutions at concentrations that are 1–2 orders of magnitude higher than those required for CD and ATR-FTIR spectroscopy in membranes. Such high concentrations are biologically less relevant in our case. This is probably due to the fact that they all contain D,L-amino acids. However, when they are bound to LPS, the spectra of the peptides and the lipopeptides could be deconvoluted. The amide I region spectra (after complete deuteration), as well as the fitted band components of the peptides when bound to LPS (obtained by deconvolution), are shown in Figure 5. The assignment of the different secondary structures to the various amide I regions was according to the values taken from other studies (41, 42, 44–47). The assignments and the relative areas of the component peaks are summarized in Table 3. The conjugation of fatty acids did not cause dramatic changes to the structure of the peptides when they are bound to LPS (Table 3 and Figure 5). Therefore, the differences seen in their biological function cannot be explained solely by differences in their structures, as will be elaborated in Discussion.

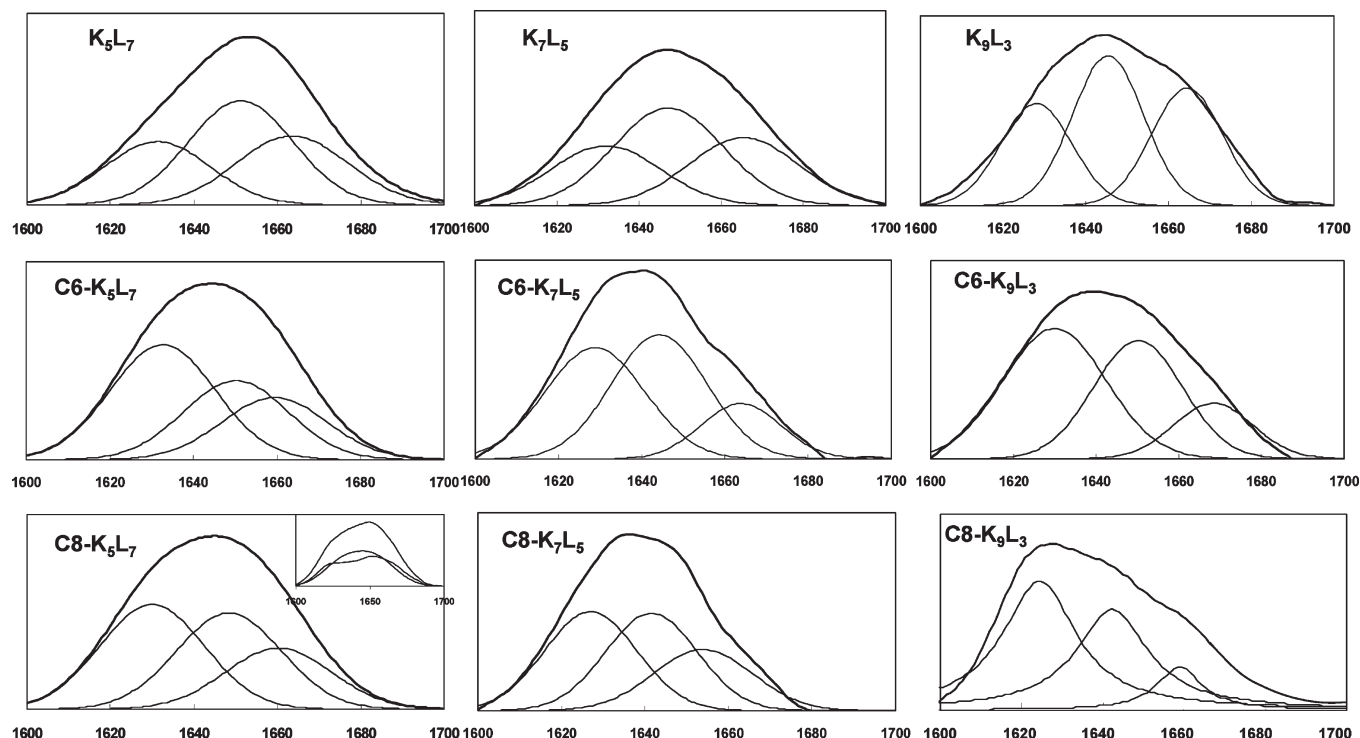


FIGURE 5: FTIR spectral deconvolution of the fully deuterated amide I band (from 1600 to 1700 cm^{-1}) of the peptides in LPS. Second derivatives were calculated to identify the positions of the component bands in the spectra. The component peaks result from curve fitting using a Gaussian line shape. The sums of the fitted components superimposed on the experimental amide I region spectra. Thick lines represent the experimental FTIR spectra; thin lines represent the fitted components. The figure presents one typical experiment of two independent experiments that were performed. The inset for C8-K₅L₇ shows an example of the spectrum of LPS alone, which served as a background (bottom line), the spectrum of C8-K₅L₇ in LPS (top line), and the spectrum of the peptide alone after subtraction of the background.

Table 3: Peptide Structure As Determined by ATR-FTIR Spectroscopy from the Deconvolution of the Amide I Bands of the Peptides Incorporated into LPS^a

| designation | β -sheet [parallel and antiparallel (%)] at 1620–1640 cm^{-1} | irregular (%) at 1640–1648 cm^{-1} | α -helix (%) at 1646–1655 cm^{-1} | 3_{10} -helix (%) at 1660–1670 cm^{-1} or β -turns (%) at 1640–1675 cm^{-1} |
|----------------------------------|---|--|--|--|
| K ₅ L ₇ | 26 \pm 0.5 (1630) | | 43 \pm 12 (1650) | 31 \pm 12 (1663) |
| C6-K ₅ L ₇ | 43 \pm 1.5 (1633) | | 32 \pm 5 (1650) | 25 \pm 5 (1660) |
| C8-K ₅ L ₇ | 39 \pm 5 (1630) | | 36 \pm 4 (1650) | 25 \pm 9 (1660) |
| K ₇ L ₅ | 29 \pm 3 (1632) | | 43 \pm 7 (1646) | 27 \pm 10 (1668) |
| C6-K ₇ L ₅ | 41 \pm 0.5 (1628) | 45 \pm 1.5 (1643) | | 15 \pm 2 (1665) |
| C8-K ₇ L ₅ | 39 \pm 2 (1627) | 37 \pm 0.3 (1642) | | 24 \pm 2 (1655) |
| K ₉ L ₃ | 28 \pm 7 (1628) | | 46 \pm 0.3 (1649) | 28 \pm 3 (1667) |
| C6-K ₉ L ₃ | 43.5 \pm 5 (1630) | | 43 \pm 5 (1650) | 14 \pm 2 (1668) |
| C8-K ₉ L ₃ | 47 \pm 5 (1625) | 40 \pm 6 (1644) | | 13 \pm 2 (1660) |

^aThe results represent the mean of the deconvolution results of at least two independent experiments.

Visualizing the Aggregates of the Peptides and Lipopeptides and Their Effect on the Morphology of LPS in Suspension. We visualized three representative peptides and lipopeptides alone and after their interaction with LPS. The list of the peptides includes the active C8-K₅L₇ and two nonactive ones, K₅L₇ and C8-K₉L₃ (at the peptide:LPS ratio used). Note that we used two methods for staining. The first was PTA, which allowed us to visualize the peptides's aggregates [and also the intact bacteria (Figure 1)], but not LPS. The second stain was uranyl acetate, which allowed visualization of LPS but not the peptides' aggregates. In buffer, both C8-K₅L₇ and C8-K₉L₃ formed nanostructures that resemble micelles (panels A and B of Figure 6, respectively). In contrast with the acylated peptides, the unmodified K₅L₇ did not oligomerize in solution and therefore is not shown. When added to LPS suspension, the two inactive peptides, K₅L₇ and C8-K₉L₃, did not change the morphology of LPS

but, rather, induced dense clusters (Figure 6D,F). In contrast, C8-K₅L₇ changed the morphology of the LPS from fibers to vesicle-like structures (Figure 6E).

DISCUSSION

Of more than 1000 natural AMPs with potent antibacterial activity, only a limited number were investigated for their mode of interaction with LPS and how this interaction affects their antibacterial activity and their ability to block LPS-induced cytokine secretion by immune cells (5, 9, 12, 14, 28, 39, 48, 49). Here we used a group of 12-amino acid peptides and their fatty acid analogues composed of D- and L-isomers of Lys and Leu. Changing the ratio between Lys and Leu and attaching short fatty acids to the N-terminus of the peptides enabled us to gradually change the ratio between their hydrophobicities and their net positive charges. Since both active and nonactive

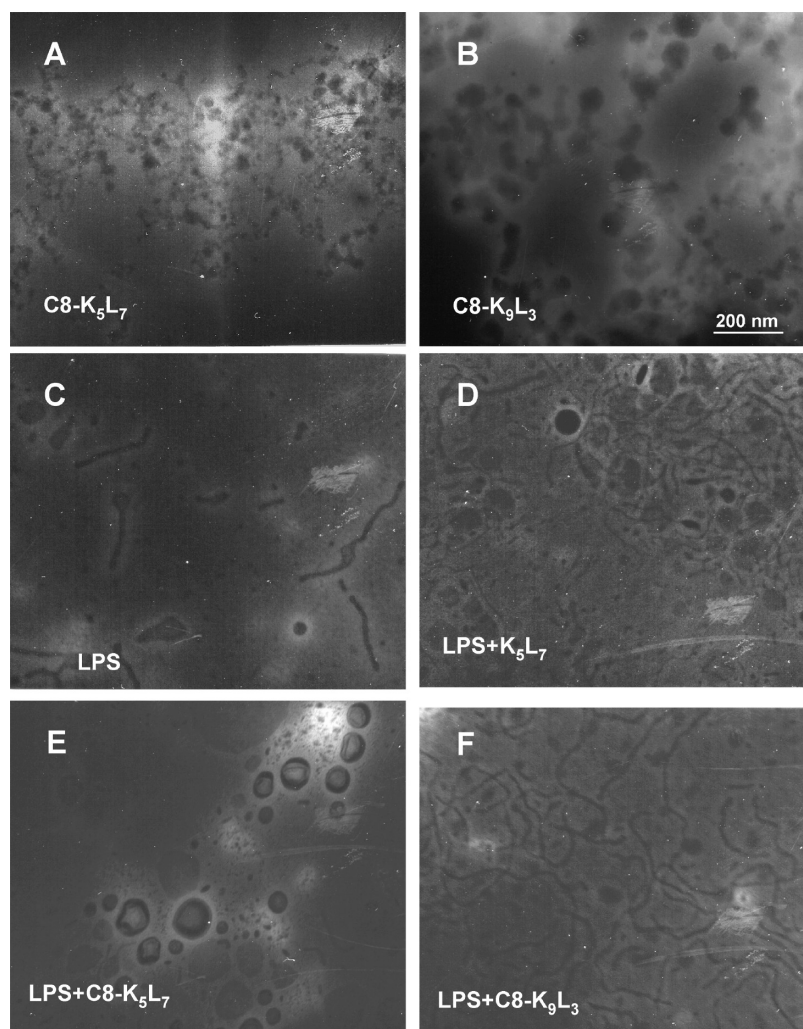


FIGURE 6: Visualization of peptides' oligomerization and their effect on LPS aggregates. (A and B) Electron micrographs of a negatively stained peptide suspension (100 μ M) in PBS. Samples of peptides were negatively stained with 2% phosphotungstic acid (pH 6.8). (C) Electron micrograph of a LPS suspension (1 mg/mL) in PBS. (D–F) Electron micrographs of the effect of the peptides on the aggregation state of LPS in suspension. All samples were negatively stained with uranyl acetate (1%). The EM image of K_5L_7 is not shown since no micelles were detected.

peptides have overall similar components of structures within LPS (Figure 5), we can assume that the differences in their activities are mainly due to differences in their charge and hydrophobicity. This hydrophobicity is an important property, enabling these AMPs to permeate the outer membrane of bacteria and to kill the bacteria, concomitant with the ability to neutralize LPS-induced endotoxic shock. However, the contribution of hydrophobicity to these two functions is not the same.

Effect of Hydrophobicity on the Antibacterial Activity of the Peptides. We found that when the structures of the peptides are not significantly different, the antibacterial activity of the peptides correlates linearly with their hydrophobicity (Figure 4A). K_5L_7 is more potent against bacteria compared with K_7L_5 and K_9L_3 (Table 2 and Figure 4A). Furthermore, attachment of hexanoic or octanoic fatty acids to the peptides significantly increased their antimicrobial activity, with a minor effect on their cell selectivity. In addition, the data point to a minimal relative hydrophobic threshold [corresponding to $\sim 30\%$ acetonitrile required to elute the peptide from a C18 column (Table 1)], below which the peptides are inactive. Note that although the resulting lipopeptides are highly oligomerized and form micelles, as revealed by negative staining EM (Figure 6), they are more

active compared with their nonacylated parental peptides. This is in contrast with previous studies in which increasing the hydrophobicity of AMPs (induced by amino acid substitution or by attachment of fatty acids) increased their α -helical structure content, which in turn induced their oligomerization. In these cases, a high degree of oligomerization significantly reduced their antimicrobial activity (50–54). A plausible explanation is that in this study oligomerization was most probably due to fatty acid micellization, since short peptides containing both D- and L-amino acids are not highly structured and therefore tend to remain as monomers. These fatty acid micelles could dissociate easily upon their interaction with the lipid A part of bacterial LPS and allow the lipopeptide to traverse into the inner target phospholipid membrane. However, in the second case, oligomerization was also induced by the α -helical peptidic chains, which makes it difficult for them to dissociate and traverse the LPS layer. The cutoff size of porins is ~ 1500 Da, and therefore, AMPs can potentially permeate through porins, too. However, since the potent antibacterial peptides listed in Table 2 are also those that are efficient in permeabilizing LPS (Figure 3), it is more reasonable to assume that they traverse directly through the LPS. Note also that in contrast with what we have found with the new series of peptides, most if not all reports revealed that an increase in the

net positive charge increases antimicrobial activity and selectivity toward bacteria compared with erythrocytes.

To further correlate between the antibacterial activity and the mode of interaction of the peptides with LPS, we investigated their ability to dissipate an artificial diffusion potential created in LPS LUVs (Figure 3). The data revealed a direct correlation between this function and both their antimicrobial activity and their hydrophobicity. Hydrophobicity seems to be one of the major properties that enables the new peptides to traverse the LPS barrier and to reach the inner cytoplasmic membrane.

Effect of Hydrophobicity on the Ability of the Peptides To Neutralize LPS. Peptides' hydrophobicity, encountered either with an increase in the ratio of Leu to Lys or by the attachment of fatty acids, increased the potency of the peptides to inhibit LPS-induced macrophage activation measured by TNF- α secretion (Figure 2). K₅L₇ and K₇L₅, but not K₉L₃, reduced the extent of TNF- α secretion (~30% inhibition after treatment with 5 μ M peptide). Further increasing the hydrophobicity of the peptides by attaching fatty acids to their N-termini resulted in an additional increase in their LPS neutralizing activity (Figure 2). Note that previous studies have shown that both bactericidal and anti-LPS activities of 18-amino acid analogues of LL37 could be augmented via substitution of hydrophilic amino acids for hydrophobic and cationic amino acids (39, 49). Although not tested in those studies, such amino acid substitutions should cause other changes in the peptides' properties, such as the amphipathic structure as well as the oligomeric state in solution and in LPS. In another study, it was shown that N-terminal acylation of a lactoferricin-derived peptide, LF11, with lauric acid (C12), greatly increased its LPS neutralizing activity compared with that of the nonacylated peptide. Interestingly, however, LF11 has a specific binding site for lipid A, which is crucial for its function (40), whereas the interactions reported in this study are controlled solely by a bulk of electrostatic and hydrophobic interactions between the peptides and LPS. This might explain why both LF11 and its acylated analogue induced a similar effect on LPS: converting the mixed unilamellar/nonlamellar aggregate structure of lipid A into a multilamellar one, although with a higher potency for the acylated analogue (28).

Here, plotting the relative hydrophobicity of the peptides versus their ability to neutralize LPS revealed that peptides within a range of certain hydrophobicities showed similar LPS neutralizing potency (Figure 4C). This differs from the linear correlation found between hydrophobicity and antibacterial activity (Figure 4A) or hydrophobicity and the ability to dissipate the diffusion potential within LPS vesicles (Figure 4B). Because of the diversity in the sequences of the peptides, it is more reasonable to assume that the active peptides use nonspecific electrostatic and hydrophobic interactions when bound to LPS, rather than a ligand–receptor-like interaction, like the interaction of the membrane active peptide with phospholipid membranes (37, 38). These interactions caused a physical change in the properties of LPS as revealed by using negative staining electron microscopy (Figure 6). These data show that fatty acid conjugation caused the resulting lipopeptides to form micelle-like structures with different morphologies (Figure 6). Furthermore, when added to LPS, the peptides had different effects on the morphology of the oligomers. The two relatively inactive peptides, C8-K₅L₃ and K₅L₇, preserved the fiberlike structure of LPS but caused high levels of condensation in these fibers (Figure 6D,E). In contrast, the highly active C8-K₅L₇ induced a change in the

LPS structure and transformed it to both small and large micelles with an overall morphology that differs from that of the lipopeptide or LPS by itself (Figure 6F). Increasing or decreasing the size of LPS micelles upon their interaction with LPS neutralizing peptides has been reported previously (55–58).

In summary, using a new series of diastereomeric membrane-active peptides in which their structure is not altered significantly upon modification reveals that increasing the ratio between hydrophobicity and the net positive charge increases both antimicrobial and LPS neutralization activities, but with different modes of contributions. Besides adding important information regarding AMP parameters involved in antimicrobial and anti-LPS activities, the findings that the diastereomers are not hemolytic suggest them as potential templates for the development of simple molecules that include both types of functions.

REFERENCES

1. Zasloff, M. (2002) Antimicrobial peptides of multicellular organisms. *Nature* 415, 389–395.
2. Hancock, R. E., and Sahl, H. G. (2006) Antimicrobial and host-defense peptides as new anti-infective therapeutic strategies. *Nat. Biotechnol.* 24, 1551–1557.
3. Boman, H. G. (1991) Antibacterial peptides: Key components needed in immunity. *Cell* 65, 205–207.
4. Bulet, P., Stocklin, R., and Menin, L. (2004) Anti-microbial peptides: From invertebrates to vertebrates. *Immunol. Rev.* 198, 169–184.
5. Radek, K., and Gallo, R. (2007) Antimicrobial peptides: Natural effectors of the innate immune system. *Semin. Immunopathol.* 29, 27–43.
6. Scott, M. G., and Hancock, R. E. (2000) Cationic antimicrobial peptides and their multifunctional role in the immune system. *Crit. Rev. Immunol.* 20, 407–431.
7. Bowdish, D. M., Davidson, D. J., Scott, M. G., and Hancock, R. E. (2005) Immunomodulatory activities of small host defense peptides. *Antimicrob. Agents Chemother.* 49, 1727–1732.
8. Bowdish, D. M., and Hancock, R. E. (2005) Anti-endotoxin properties of cationic host defence peptides and proteins. *J. Endotoxin Res.* 11, 230–236.
9. Rosenfeld, Y., and Shai, Y. (2006) Lipopolysaccharide (endotoxin)-host defense antibacterial peptides interactions: Role in bacterial resistance and prevention of sepsis. *Biochim. Biophys. Acta* 1758, 1513–1522.
10. Kandler, K., Shaykhiev, R., Kleemann, P., Kleszcz, F., Lohoff, M., Vogelmeier, C., and Bals, R. (2006) The anti-microbial peptide LL-37 inhibits the activation of dendritic cells by TLR ligands. *Int. Immunol.* 18, 1729–1736.
11. Mookherjee, N., Brown, K. L., Bowdish, D. M., Doria, S., Falsafi, R., Hokamp, K., Roche, F. M., Mu, R., Doho, G. H., Pistolic, J., Powers, J. P., Bryan, J., Brinkman, F. S., and Hancock, R. E. (2006) Modulation of the TLR-mediated inflammatory response by the endogenous human host defense peptide LL-37. *J. Immunol.* 176, 2455–2464.
12. Mookherjee, N., Wilson, H. L., Doria, S., Popowich, Y., Falsafi, R., Yu, J. J., Li, Y., Veatch, S., Roche, F. M., Brown, K. L., Brinkman, F. S., Hokamp, K., Potter, A., Babiuk, L. A., Griebel, P. J., and Hancock, R. E. (2006) Bovine and human cathelicidin cationic host defense peptides similarly suppress transcriptional responses to bacterial lipopolysaccharide. *J. Leukocyte Biol.* 80, 1563–1574.
13. Giacometti, A., Cirioni, O., Ghiselli, R., Mocchegiani, F., Orlando, F., Silvestri, C., Bozzi, A., Di Giulio, A., Luzi, C., Mangoni, M. L., Barra, D., Saba, V., Scalise, G., and Rinaldi, A. C. (2006) Interaction of antimicrobial peptide temporin L with lipopolysaccharide in vitro and in experimental rat models of septic shock caused by Gram-negative bacteria. *Antimicrob. Agents Chemother.* 50, 2478–2486.
14. Motzkus, D., Schulz-Maronde, S., Heitland, A., Schulz, A., Forssmann, W. G., Jubner, M., and Maronde, E. (2006) The novel β -defensin DEFB123 prevents lipopolysaccharide-mediated effects in vitro and in vivo. *FASEB J.* 20, 1701–1702.
15. Nagaoka, I., Yomogida, S., Tamura, H., and Hirata, M. (2004) Antibacterial cathelicidin peptide CAP11 inhibits the lipopolysaccharide (LPS)-induced suppression of neutrophil apoptosis by blocking the binding of LPS to target cells. *Inflammation Res.* 53, 609–622.
16. Gee, K., Kozlowski, M., and Kumar, A. (2003) Tumor necrosis factor- α induces functionally active hyaluronan-adhesive CD44 by

- activating sialidase through p38 mitogen-activated protein kinase in lipopolysaccharide-stimulated human monocytic cells. *J. Biol. Chem.* 278, 37275–37287.
17. Mukhopadhyay, S., Herre, J., Brown, G. D., and Gordon, S. (2004) The potential for Toll-like receptors to collaborate with other innate immune receptors. *Immunology* 112, 521–530.
18. Cohen, J. (2002) The immunopathogenesis of sepsis. *Nature* 420, 885–891.
19. Angus, D. C., and Wax, R. S. (2001) Epidemiology of sepsis: An update. *Crit. Care Med.* 29, S109–S116.
20. Temple, S. E., Cheong, K. Y., Almeida, C. M., Price, P., and Waterer, G. W. (2003) Polymorphisms in lymphotoxin α and CD14 genes influence TNF α production induced by Gram-positive and Gram-negative bacteria. *Genes Immun.* 4, 283–288.
21. Hancock, R. E., and Diamond, G. (2000) The role of cationic antimicrobial peptides in innate host defences. *Trends Microbiol.* 8, 402–410.
22. Scott, M. G., Davidson, D. J., Gold, M. R., Bowdish, D., and Hancock, R. E. (2002) The human antimicrobial peptide LL-37 is a multifunctional modulator of innate immune responses. *J. Immunol.* 169, 3883–3891.
23. Rosenfeld, Y., Papo, N., and Shai, Y. (2006) Endotoxin (lipopolysaccharide) neutralization by innate immunity host-defense peptides. Peptide properties and plausible modes of action. *J. Biol. Chem.* 281, 1636–1643.
24. Bommineni, Y. R., Dai, H., Gong, Y. X., Soulages, J. L., Fernando, S. C., Desilva, U., Prakash, O., and Zhang, G. (2007) Fowlcidin-3 is an α -helical cationic host defense peptide with potent antibacterial and lipopolysaccharide-neutralizing activities. *FEBS J.* 274, 418–428.
25. Mookherjee, N., and Hancock, R. E. (2007) Cationic host defence peptides: Innate immune regulatory peptides as a novel approach for treating infections. *Cell. Mol. Life Sci.* 64, 922–933.
26. Zanetti, M. (2005) The role of cathelicidins in the innate host defenses of mammals. *Curr. Issues Mol. Biol.* 7, 179–196.
27. Andra, J., Koch, M. H., Bartels, R., and Brandenburg, K. (2004) Biophysical characterization of endotoxin inactivation by NK-2, an antimicrobial peptide derived from mammalian NK-lysin. *Antimicrob. Agents Chemother.* 48, 1593–1599.
28. Andra, J., Lohner, K., Blondelle, S. E., Jerala, R., Moriyon, I., Koch, M. H., Garidel, P., and Brandenburg, K. (2005) Enhancement of endotoxin neutralization by coupling of a C12-alkyl chain to a lactoferricin-derived peptide. *Biochem. J.* 385, 135–143.
29. Banemann, A., Deppisch, H., and Gross, R. (1998) The lipopolysaccharide of *Bordetella bronchiseptica* acts as a protective shield against antimicrobial peptides. *Infect. Immun.* 66, 5607–5612.
30. Allende, D., and McIntosh, T. J. (2003) Lipopolysaccharides in bacterial membranes act like cholesterol in eukaryotic plasma membranes in providing protection against melittin-induced bilayer lysis. *Biochemistry* 42, 1101–1108.
31. Papo, N., and Shai, Y. (2005) A molecular mechanism for lipopolysaccharide protection of Gram-negative bacteria from antimicrobial peptides. *J. Biol. Chem.* 280, 10378–10387.
32. Loutet, S. A., Flannagan, R. S., Kooi, C., Sokol, P. A., and Valvano, M. A. (2006) A complete lipopolysaccharide inner core oligosaccharide is required for resistance of *Burkholderia cenocepacia* to antimicrobial peptides and bacterial survival in vivo. *J. Bacteriol.* 188, 2073–2080.
33. Rana, F. R., Macias, E. A., Sultany, C. M., Modzrakowski, M. C., and Blazyk, J. (1991) Interactions between magainin 2 and *Salmonella typhimurium* outer membranes: Effect of lipopolysaccharide structure. *Biochemistry* 30, 5858–5866.
34. Rana, F. R., and Blazyk, J. (1991) Interactions between the antimicrobial peptide, magainin 2, and *Salmonella typhimurium* lipopolysaccharides. *FEBS Lett.* 293, 11–15.
35. Farnaud, S., Spiller, C., Moriarty, L. C., Patel, A., Gant, V., Odell, E. W., and Evans, R. W. (2004) Interactions of lactoferricin-derived peptides with LPS and antimicrobial activity. *FEMS Microbiol. Lett.* 233, 193–199.
36. Piers, K. L., and Hancock, R. E. (1994) The interaction of a recombinant cecropin/melittin hybrid peptide with the outer membrane of *Pseudomonas aeruginosa*. *Mol. Microbiol.* 12, 951–958.
37. Papo, N., and Shai, Y. (2003) Can we predict biological activity of antimicrobial peptides from their interactions with model phospholipid membranes? *Peptides* 24, 1693–703.
38. Brown, K. L., and Hancock, R. E. (2006) Cationic host defense (antimicrobial) peptides. *Curr. Opin. Immunol.* 18, 24–30.
39. Nagaoka, I., Hirota, S., Niyonsaba, F., Hirata, M., Adachi, Y., Tamura, H., Tanaka, S., and Heumann, D. (2002) Augmentation of the lipopolysaccharide-neutralizing activities of human cathelicidin CAP18/LL-37-derived antimicrobial peptides by replacement with hydrophobic and cationic amino acid residues. *Clin. Diagn. Lab. Immunol.* 9, 972–982.
40. Japelj, B., Pristovsek, P., Majerle, A., and Jerala, R. (2005) Structural origin of endotoxin neutralization and antimicrobial activity of a lactoferrin-based peptide. *J. Biol. Chem.* 280, 16955–16961.
41. Byler, D. M., and Susi, H. (1986) Examination of the secondary structure of proteins by deconvolved FTIR spectra. *Biopolymers* 25, 469–487.
42. Sharon, M., Oren, Z., Shai, Y., and Anglister, J. (1999) 2D-NMR and ATR-FTIR study of the structure of a cell-selective diastereomer of melittin and its orientation in phospholipids. *Biochemistry* 38, 15305–15316.
43. Oren, Z., Ramesh, J., Avrahami, D., Suryaprakash, N., Shai, Y., and Jelinek, R. (2002) Structures and mode of membrane interaction of a short α helical lytic peptide and its diastereomer determined by NMR, FTIR, and fluorescence spectroscopy. *Eur. J. Biochem.* 269, 3869–3880.
44. Surewicz, W. K., and Mantsch, H. H. (1988) New insight into protein secondary structure from resolution-enhanced infrared spectra. *Biochim. Biophys. Acta* 952, 115–130.
45. Jackson, M., and Mantsch, H. H. (1995) The use and misuse of FTIR spectroscopy in the determination of protein structure. *Crit. Rev. Biochem. Mol. Biol.* 30, 95–120.
46. Frey, S., and Tamm, L. K. (1991) Orientation of melittin in phospholipid bilayers. A polarized attenuated total reflection infrared study. *Biophys. J.* 60, 922–930.
47. Tatulian, S. A. (2003) Attenuated total reflection Fourier transform infrared spectroscopy: A method of choice for studying membrane proteins and lipids. *Biochemistry* 42, 11898–11907.
48. Scott, M. G., Yan, H., and Hancock, R. E. (1999) Biological properties of structurally related α -helical cationic antimicrobial peptides. *Infect. Immun.* 67, 2005–2009.
49. Nagaoka, I., Kuwahara-Arai, K., Tamura, H., Hiramatsu, K., and Hirata, M. (2005) Augmentation of the bactericidal activities of human cathelicidin CAP18/LL-37-derived antimicrobial peptides by amino acid substitutions. *Inflammation Res.* 54, 66–73.
50. Avrahami, D., and Shai, Y. (2002) Conjugation of a magainin analogue with lipophilic acids controls hydrophobicity, solution assembly, and cell selectivity. *Biochemistry* 41, 2254–2263.
51. Malina, A., and Shai, Y. (2005) Conjugation of fatty acids with different lengths modulates the antibacterial and antifungal activity of a cationic biologically inactive peptide. *Biochem. J.* 390, 695–702.
52. Makovitzki, A., Avrahami, D., and Shai, Y. (2006) Ultrashort antibacterial and antifungal lipopeptides. *Proc. Natl. Acad. Sci. U.S.A.* 103, 15997–16002.
53. Chen, Y., Guarnieri, M. T., Vasil, A. I., Vasil, M. L., Mant, C. T., and Hodges, R. S. (2007) Role of peptide hydrophobicity in the mechanism of action of α -helical antimicrobial peptides. *Antimicrob. Agents Chemother.* 51, 1398–1406.
54. Radziszewsky, I. S., Kovachi, T., Porat, Y., Ziserman, L., Zaknoon, F., Danino, D., and Mor, A. (2008) Structure-activity relationships of antibacterial acyl-lysine oligomers. *Chem. Biol.* 15, 354–362.
55. Andra, J., Howe, J., Garidel, P., Rossle, M., Richter, W., Leiva-Leon, J., Moriyon, I., Bartels, R., Gutsmann, T., and Brandenburg, K. (2007) Mechanism of interaction of optimized Limulus-derived cyclic peptides with endotoxins: Thermodynamic, biophysical and microbiological analysis. *Biochem. J.* 406, 297–307.
56. Andra, J., Lamata, M., Martinez de Tejada, G., Bartels, R., Koch, M. H., and Brandenburg, K. (2004) Cyclic antimicrobial peptides based on Limulus anti-lipopolysaccharide factor for neutralization of lipopolysaccharide. *Biochem. Pharmacol.* 68, 1297–1307.
57. Howe, J., Andra, J., Conde, R., Iriarte, M., Garidel, P., Koch, M. H., Gutsmann, T., Moriyon, I., and Brandenburg, K. (2007) Thermodynamic analysis of the lipopolysaccharide-dependent resistance of Gram-negative bacteria against polymyxin B. *Biophys. J.* 92, 2796–2805.
58. Rosenfeld, Y., Sahl, H. G., and Shai, Y. (2008) Parameters involved in antimicrobial and endotoxin detoxification activities of antimicrobial peptides. *Biochemistry* 47, 6468–6478.